The role of diffusion-weighted imaging MRI in differentiation between benign and malignant axillary lymphadenopathy in clinically TNM stages I and II breast cancer

Mostafa T. Hussein[a], Badawy M. Ahmed[b], Omran K. Qenawy[c], Abeer H. Ali[c], Esraa M.A. Omar[d]

Departments of [a]Diagnostic Radiology and [b]Surgical Oncology, Faculty of Medicine, Assiut University Departments of [c]Radiodiagnosis, Interventional Radiology and [d]Diagnostic Radiology, Assiut University Hospitals, Assiut, Egypt

Correspondence to Esraa M.A. Omar, M.B.B.Ch., Resident at Diagnostic Radiology Department, Assuit University Hospitals, Assiut, Egypt. Zipcode: 71111; Tel.: 01092700918; e-mail: esraaahdy91@gmail.com

Received 07 July 2020
Revised 17 August 2020
Accepted 27 January 2021
Published 09 October 2021

Journal of Current Medical Research and Practice
2021, 6:257–263

Objective

To investigate diffusion-weighted imaging (DWI) in differentiation of metastatic from nonmetastatic axillary lymph nodes (ALNs) in clinically stages I and II breast cancer.

Patients and methods

A total of 255 ALNs from 30 female patients with histologically proved breast cancer were assessed by 1.5 T scanner. DWI was implemented at *b* values of 50, 400, and 800 s/mm^2. Short-axis diameter, presence of fatty hilum, and apparent diffusion coefficient (ADC) values (minimum and maximum and mean) of metastatic and nonmetastatic ALNs were compared. Cutoff ADC values to discriminate between benign and malignant ALNs were analyzed with receiver coefficient characteristic (receiver operating characteristic) curves.

Results

The final histopathological examination revealed 69.4% (n = 177) metastatic and 30.6% (n = 78) nonmetastatic ALNs. There was no statistically significant difference in short-axis diameter between the two groups (P = 0.82). However, there was a significantly correlation between loss of fatty hilum and presence of metastases (P < 0.001), and ADC values [$0.85 \pm 0.35 \times 10^{-3}$ mm^2/s vs. $1.28 \pm 0.51 \times 10^{-3}$ mm^2/s (ADC minimum), $1.15 \pm 5.30 \times 10^{-3}$ mm^2/s vs. $1.937 \pm 0.78 \times 10^{-3}$ mm^2/s (ADC maximum), and $0.90 \pm 0.44 \times 10^{-3}$ mm^2/s vs. $1.32 \pm 0.55 \times 10^{-3}$ mm^2/s (ADC mean)], of metastatic ALNs were significantly lower than those of nonmetastatic ALNs (P < 0.001). The optimal mean ADC cutoff value for differentiation between metastatic and nonmetastatic ALNs was less than 1.22×10^{-3} mm^2/s, which had a higher specificity (77%) and accuracy (82.4%) as compared with ADC minimum and ADC maximum.

Conclusion

DWI-MRI and ADC values are promising imaging methods that can assess metastatic ALNs in early breast cancer with high sensitivity, specificity, and accuracy.

Keywords:

axillary lymph nodes, breast cancer, diffusion-weighted imaging-MRI, metastasis

J Curr Med Res Pract 6:257–263

2357-0121

Introduction

Breast cancer is the most commonly diagnosed cancer among women, with ~ 182 000 women diagnosed with breast cancer annually in the United States [1].

Accurate prediction and early diagnosis of the metastatic status of axillary lymph nodes (ALNs) is very important to create a plan of treatment and grading for patients with early stages of breast cancer [2].

Nowadays, MRI as a noninvasive method is used for preoperative grading of metastatic ALNs, which has high sensitivity and specificity [3].

Diffusion-weighted imaging (DWI-MRI) is a noninvasive technique that works on Brownian motion of water molecules. Apparent diffusion coefficient (ADC) value is calculated by using two or more diffusion images, which is depended on certain parameters such as size of cell, inside and outside cellular volume fraction, and cell membrane permeability [4].

In many organs, increase of cellularity of malignant cells to benign causes reduction in the amount of ADC. So, metastatic ALNs have low ADC value [5].

In general, DW-MRI has become an emerging technique for discrimination of benign from malignant ALN in short time [6]. The aim of these study is to investigate the feasibility of DWI-MRI in differentiation of metastatic from nonmetastatic ALNs.

Patients and methods

Patients

This randomized prospective study was performed in cooperation between Surgical Oncology Department, South Egypt Cancer Institute, and MRI unit at Radiology Department, Assiut University Hospital, Assiut University, from May 2017 to May 2018 and carried out on 30 female patients with histologically proved breast cancer TNM stages I and II.

Approval of local ethics committee of Faculty of Medicine, Assiut University, was obtained under IRB number 17101132. The recruited patients were informed about the study aims, and all patients signed informed consent.

Inclusion criteria

Patients in different ages, proved to have breast cancer with histological examination in clinically TNM stages I and II breast cancer, were included.

Exclusion criteria

The following were the exclusion criteria:

(1) Patients with any general contraindication to MRI such as presence of any paramagnetic substance or in severely ill patients or claustrophobia.
(2) Patients undergoing any type of neo-adjuvant, chemotherapy, immune, or endocrine therapy.
(3) Patients with history of axillary surgery or treatment.
(4) Patients with other causes of lymphadenopathy rather than breast cancer.
(5) Patients unfit or refusing surgery.

MRI technique

MRI was performed on a 1.5 T scanner (Sempra, Siemens, Erlangen Germany). The patient was placed in the prone position with both breasts placed adequately in double breast coil (four-channel phased array coil).

Patient position

The MRI was performed with the patient in the prone position, head first with both arms extending in front, lying on a platform placed in the MR imager that allows the breast to extend dependently and unfolded from the patient. Prone patient positioning minimizes the effects of respiratory movement.

MRI protocol

(1) Axial T2-weighted fast spin echo sequence: TR = 3840 ms, TE = 81 ms, slice thickness = 3.5 mm, and matrix = 448 × 448.
(2) Coronal T2-weighted fast spin echo sequence: TR = 3840 ms, TE = 81 ms, slice thickness = 3.5 mm, and matrix = 448 × 448.
(3) Short tau inversion recovery – axial: TR = 8540 ms, TE = 59 ms, TI = 170 ms, slice thickness = 3.5 mm, and matrix = 320 × 314.

Sensitizing diffusion gradients were done with b value of 50, 400, and 800 s/mm^2 with the following parameters: TR: 7700 ms, TE: 89 ms, matrix: 192 × 192 pixels, and slice thickness 5 mm to reduce motion artifact. Phase encoding direction was AP in the axial plane.

Image analysis

All MRI were reviewed by two radiologists. We selected the ALNs with short axis larger than 5 mm. In our study, morphological MRI analysis was performed on T2W image. Suspicious morphological criteria of metastatic ALNs included short-axis diameter more than 10 mm, loss of fatty hilum, irregular margins or apparent speculation, and diffusion restriction (reference). For the assessment of ADC value, a round or elliptical region of interest (ROI) was drawn manually with greatest diameter to cover nearly the inner margin of LN on the central slice of each LN on ADC map. Trying to avoid addition of the margins at ROI, T2W-FSE images were selected as an anatomical reference.

All the ADC values were averaged from three-time measurement and expressed as the mean ± SD. Three ADC values (minimum ADC, maximum ADC, and mean ADC) were calculated for all selected ALNs.

Surgical procedure and pathological analysis

Within 2 weeks after MRI examination, all patients underwent definitive surgery and received a definite pathological diagnosis. All pathological samples were interpreted by one or more expert pathologists in breast pathology, who were blinded to the MRI results. Correlation between the diffusion MR finding and pathological reports for these selected LNs was performed.

Statistical analysis

The analysis of data was performed to assess statistical significant variances. The loss of fatty hila, mean short axis, and the ADC values (minimum and maximum) receiver operating characteristic (ROC) curves were plotted to discriminate benign from metastatic ALNs, with calculation of accuracy, specificity, sensitivity, and area under the curve. Accuracy, specificity, and sensitivity of data achieved by ADC-DWI examination in discriminating ALNs were evaluated using the histopathological results as the gold standard. Statistical analyses were performed by using SPSS, version 20 (IBM, Armonk, New York, USA).

Results

This study was prospectively performed on 30 women with histologically proven breast cancer with the main cancer types consisted of 20 (66.67%) invasive ductal carcinoma and 10 (33.33%) lobular carcinoma. Their age ranged from 30 to 66 years, with a mean age of 44.8 ± 14.8 years, and the affected side was left in nine patients, right in eight patients, and bilateral in 13 patients.

We examined the LNs on a node-by-node basis. A total of 255 LNs were coordinated radiologically and pathologically and included in the analysis, where 177 (69.4%) of examined LNs were malignant. Tables 1–4 show morphological and radiological findings of examined ALNs based on the pathological evaluation. It was noticed that the majority of malignant ALNs lost fatty hilum (79.7%) and had irregular margin (71.2%), whereas each of loss of fatty hilum and irregular margin presented in only six cases of benign ALNs (P < 0.05) (Fig. 1).

Both types of LNs had no significant differences regarding the short-axis diameter (8.23 ± 3.77 mm for malignant LNs vs. 8.04 ± 2.72 mm for benign LNs; P = 0.82).

Regarding ADC value, it was noticed that malignant ALNs had significantly lower ADC values in comparison with benign ALNs, where the mean ADC was 0.90 ± 0.44 and 1.32 ± 0.55 × 10^{-3}/mm²/s in the case of malignant LNs and benign LNs, respectively (P = 0.01) (Figs. 2 and 3). Among the surgically resected ALNs, there was a high restriction in DWI in all malignant LNs and 24 (30.8%) of benign LNs. Low restriction was presented in 54 (69.2%) of the benign ALNs.

Diagnostic performance of morphological features in diagnosing malignant ALNs (Fig. 4).

It was noticed that loss of hilum had 80% sensitivity and 92.3% specificity in prediction of malignant LNs, with an area under the curve of 0.8 and P value less than 0.001, whereas irregular margin had 71% sensitivity and 92% specificity in prediction of malignant LNs, with an area under the curve of 0.82 and P value less than 0.001.

Diagnostic performance of ADC in diagnosing malignant ALNs is shown in Fig. 5.

Table 1 Characteristics of examined lymph nodes based on pathological diagnosis

	Malignant LNs (n=177)	Benign LNs (n=78)	P
Morphology			
Loss of fatty hilum	141 (79.7)	6 (7.7)	<0.001
Irregular margin	126 (71.2)	6 (7.7)	<0.001
Axis diameter (mm)	8.23±3.77	8.04±2.72	0.82
ADC value (10^{-3}/mm²/s)			
Minimum	0.85±0.35	1.28±0.51	0.01
Maximum	1.15±5.30	1.93±0.78	0.04
Mean	0.90±0.44	1.32±0.55	0.01
Restriction			
Low	0	54 (69.2)	<0.001
High	177 (100)	24 (30.8)	

Data was expressed in form of frequency (percentage), mean±SD. ADC, apparent diffusion coefficient; LNs, lymph nodes. P<0.05.

Table 2 Diagnostic performance of morphology in diagnosing malignant lymph nodes

	Loss of hilum (%)	Irregular margin (%)
Sensitivity	80	71
Specificity	92.3	92
Positive predictive value	96	96
Negative predictive value	67	59
Accuracy	83.5	77.6
Area under curve	0.86	0.82
P	<0.001	< 0.001

P<0.05.

Table 3 Diagnostic performance of apparent diffusion coefficient in diagnosing malignant lymph nodes

	Maximum ADC (%)	Minimum ADC (%)	Mean ADC (%)
Sensitivity	84.44	83	85
Specificity	65.40	35	77
Positive predictive value	85	74	89.3
Negative predictive value	68	47	67
Cut off point (10^{-3}/mm²/s)	<1.62	<0.92	<1.22
Accuracy	78.8	68	82.4
Area under the curve	0.78	0.55	0.82
P	0.01	0.03	0.01

ADC, apparent diffusion coefficient. P<0.05.

Table 4 Diagnostic performance of high restriction in diagnosing malignant lymph nodes

	Indices (%)
Sensitivity	100
Specificity	69
Positive predictive value	88
Negative predictive value	100
Accuracy	90.5
Area under curve	0.85
P	<0.001

P<0.05.

Figure 1

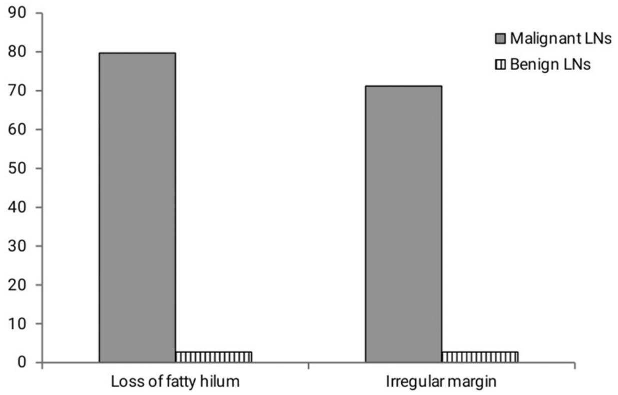

Morphological features of examined LNs based on pathological diagnosis. LN, lymph node.

Figure 2

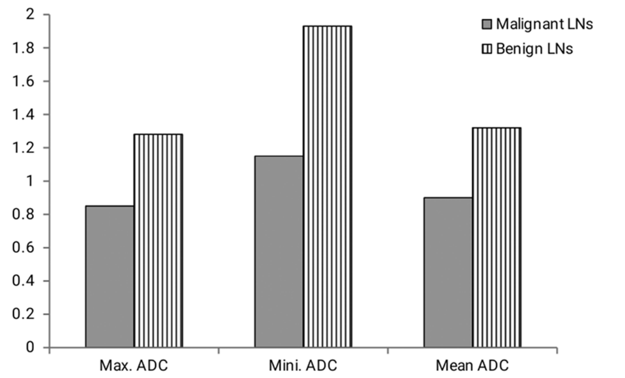

ADC values of examined LNs based on pathological diagnosis. ADC, apparent diffusion coefficient; LN, lymph node.

Figure 3

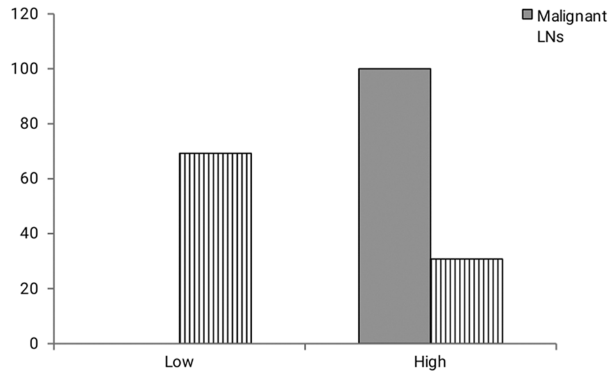

Restriction in DWI of examined LNs based on pathological diagnosis. DWI, diffusion-weighted imaging; LN, lymph node.

Figure 4

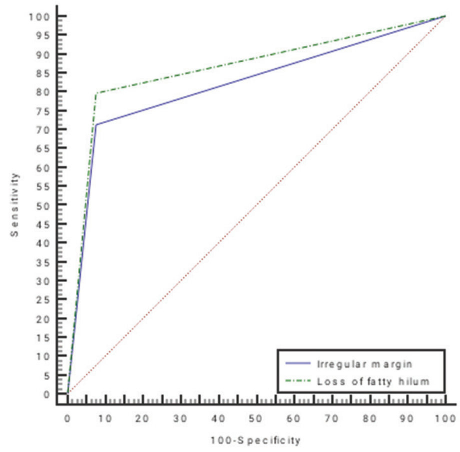

Diagnostic performance of morphological features in diagnosing malignant LNs. LN, lymph node.

Our results based on ROC curve analysis showed that the maximum ADC value at cutoff point less than $1.62 \times 10^{-3} mm^2/s$ had 84.44% sensitivity and 65.40% specificity, with an area under the curve of 0.78 and *P* value of 0.01; the minimum ADC value, at cutoff point less than $0.92 \times 10^{-3} mm^2/s$ had 83% sensitivity and 35% specificity, with an area under the curve of 0.55 and *P* value of 0.04; and the mean ADC value, at cutoff point less than $1.22 \times 10^{-3} mm^2/s$ had 85% sensitivity and 77% specificity, with an area under the curve of 0.59 and *P* value of 0.01.

While assessing the diagnostic performance of high restriction for diagnosing the malignant ALNs (Fig. 6), it was noticed that high restriction in DWI had 100% sensitivity and 69% specificity with an area under the curve of 0.85 and *P* value less than 0.001.

Discussion

ALNs with short axis more than 10 mm are a positive traditional indicator for malignancy [7]. The studies by Razek *et al.*[8] and Chung *et al.*[9] reported metastatic ALNs are larger than nonmetastatic types. However, many other authors such as Ismail *et al.*[10] stated there is no significant relationship between the size of the LNs and the presence of metastasis. Moreover, we found no significant difference in the short-axis diameter between metastatic (8.23 ± 3.77 mm) and benign nodes (8.04 ± 2.72 mm), and there is an overlap in the diameter of the short axis between both groups ($P = 0.82$).

Some studies have reported the loss of fatty hilum as a predictor for metastatic ALNs [11]. We also found similar results; therefore, there was a significant correlation between loss of fatty hilum of ALNs and presence of metastatic nodes ($P < 0.001$). However, some other studies reported that both inflammatory and malignant LNs have high signal intensity on DWI, which makes it difficult to identify [12,13].

We found that there was a significant correlation between the irregular margin of ALNs and the presence

Figure 5

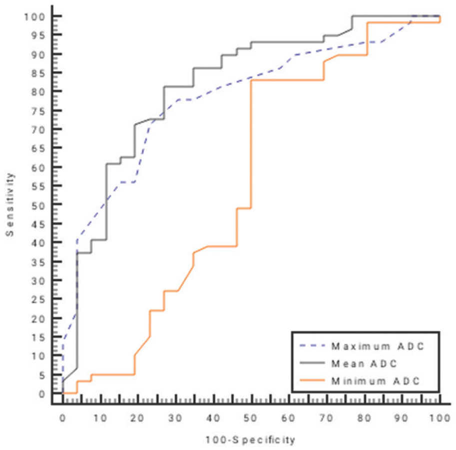

Diagnostic performance of ADC value in diagnosing malignant LNs. ADC, apparent diffusion coefficient; LN, lymph node.

Figure 6

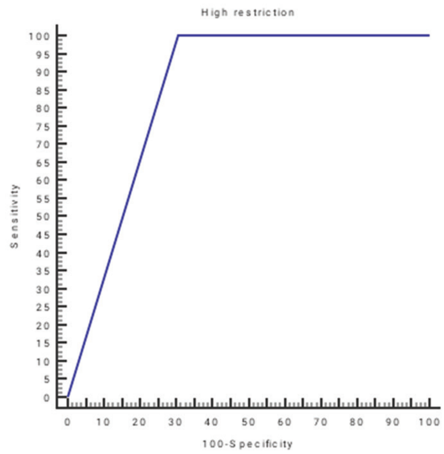

Diagnostic performance of high restriction in diagnosing malignant LN. LN, lymph node.

of metastatic nodes ($P < 0.001$), where 126 ALNs had irregular margin from total malignant ALNs (177), and only six ALNs from total benign ALNs ($n = 78$). The irregular margin showed 71, 92, and 77% as sensitivity, specificity, and accuracy, respectively, in the prediction of malignant ALNs.

We found that 126 ALNs from total of 177 malignant LNs had both loss of fatty hilum and irregular outline and 66 ALNs from total of 78 benign LNs had preserved fatty hilum and smooth margin.

In the present study, the high signal intensity of the ALNs on DWI was detected in 201 nodes (177 with and 24 without metastasis), whereas low signal intensity was detected in 58 LNs without metastasis. The presence of high signal on DWI in metastatic LNs was found to be statistically significant ($P = 0.001$), and this was in agreement with Ismail *et al.* [10]. However, Wang *et al.*[12] in their study on rabbit models found that both the metastatic and the inflammatory LNs presented with high signal intensity on DWI and that there was no statistically significant difference comparing the signal intensity on DWI between inflammatory and metastatic LNs.

They concluded that visual assessment of DWI to differentiate metastatic from inflammatory ALNs was difficult because both groups showed high signal intensities on DWI [5].

Measuring the ADC value yielded quantitative assessment of the water diffusivity in the tissue, and the larger the b value is, the greater the degree of signal attenuation from the motion of water molecules is [14]. In the study of Wang *et al.* [12], they used a high b value of 800 s/mm^2, and they assumed that high b value could evaluate water diffusion more exactly and eliminate the effects of capillary perfusion.

Moreover, in our study, the obtained ADC values were significantly lower for ALNs with metastasis than those without metastasis. Many other previous studies had published the same results [8,10,12], which gave an overlap between both groups and the explanation for this overlap was they found that not all malignant LNs were totally replaced by tumor cells, resulting in areas of metastasis with lower ADC and another area without metastasis with higher ADC, and also the ROI of the ADC in a LN may be heterogeneous, containing metastatic and nonmetastatic portions.

On the contrary, in nonmetastatic LN, diffusion of water molecules may be limited by inflammatory cell infiltration, reactive hyperplasia, or fibrous connective tissue proliferation, which leads to decrease in ADC value [7].

The biophysical basis for these lower ADC values in malignant tumors is still poorly understood. According to previous data in the literature, potential reasons for the decreased ADC values within malignancies were probably related to a combination of higher cellularity, cellular polymorphism, and diminished extracellular space, all contributing to reduced motion of water. Thus, malignant lesions, such as metastatic LNs, tend to show low ADC values; nontumor tissue changes with low cellularity, such as inflammation and fibrosis, are expected to show strong contrast with tumor masses.

In our study, obtained mean ADC values were significantly lower for metastatic ALNs than nonmetastatic type ($0.90 \pm 0.44 \times 10^{-3}$ mm^2/s vs.

$1.32 \pm 0.55 \times 10^{-3}$ mm^2/s); many other prior studies had similar results [8,10,12].

The cutoff value of mean ADC for discriminating benign from malignant ALNs was 1.22×10^{-3} mm^2/s, with a sensitivity of 85%, specificity of 77%, and accuracy of 82.4%, which is virtually similar to the results of Yamaguchi *et al.*[15] and Razek *et al.* [8]. The minimum and maximum ADC values of metastatic ALNs were $0.85 \pm 0.35 \times 10^{-3}$ mm^2/s and $1.15 \pm 5.30 \times 10^{-3}$ mm^2/s, respectively. Moreover, they were lower than those of nonmetastatic ALNs, which were $1.28 \pm 0.51 \times 10^{-3}$ mm^2/s and $1.93 \pm 0.78 \times 10^{-3}$ mm^2/s, respectively.

In this study, we compared the diagnostic value of the mean, minimum, and maximum ADC. Based on ROC analysis, the mean and minimum ADC values showed near sensitivity (85 and 83%, respectively), but the mean ADC had higher accuracy (82.4%) and specificity (77%) compared with minimum and maximum ADC.

There was a wide difference in the mean and cutoff value of ADC between the different studies. Some studies have demonstrated this difference to that the ADC value had been affected by many factors, such as the magnetic field, MRI acquisition parameters, location, size and area of ROI, patient age, as well as the body temperature [16].

Few studies, such as Kamitani *et al.* [6], reported the opposite results; in their studies, the ADC value of metastatic ALNs was higher than that of nonmetastatic one. These results may be explained by the difference in the histological types, the variation within LNs at the cellular level, and also heterogeneous ROI. In the necrotic tissue, cell density is low, so the ADC value becomes higher. Moreover, ADC value may increase in LNs with inflammation owing to edema if there is no inflammatory cell infiltration, reactive hyperplasia, and fibrous connective tissue proliferation [12,15].

Study limitations

In this study we faced a limitation:

First, sensitivity of MRI in detecting LNs less than 5 mm is low due to the limited resolution of DWI-MRI, so ALNs smaller than 5 mm were not evaluated. SLNB is currently the most accurate method to exclude small micrometastatic ALNs in breast cancer. Further improvement, to get higher spatial resolution DWI images and more anatomical details, 3.0 T MRI is recommended to allow the study of smaller nodules.

Second, ALNs were not located in the center of the field of the coil. Therefore, use of coils for ALNs is recommended for better evaluation, so axillary coil could be ideal.

Third, DWI are very sensitive to artifacts such as motion, susceptibility, or chemical shift, which makes it difficult to discover of lesions on DWI.

The fourth limitation was the low number of patients. Additional studies with large number of participants will increase the accuracy of the results of DWI-MRI and guide physicians involved in the diagnosis, treatment, and follow-up of patients with breast cancer.

Conclusion

In conclusion, our results indicated that DWI-MRI and ADC values are promising imaging methods that can assess metastatic ALNs in breast cancer with higher sensitivity, specificity, and accuracy.

Financial support and sponsorship

Nil.

Conflicts of interest

There are no conflicts of interest.

References

1 Jemal A, Siegel R, Ward E, Hao Y, Xu J, Murray T, *et al.* Cancer statistics, 2008. CA Cancer J Clin 2008; 58:71–96.

2 Chung J, Youk JH, Kim J-A, Gweon HM, Kim E-K, Ryu YH, *et al.* Role of diffusion-weighted MRI: predicting axillary lymph node metastases in breast cancer. Acta Radiol 2014; 55:909–916.

3 Damrauer JS, Hoadley KA, Chism DD, Fan C, Tiganelli CJ, Wobker SE, *et al.* Intrinsic subtypes of high- grade bladder cancer reflect the hallmarks of breast cancer biology. Proc Natl Acad Sci 2014; 111:3110–3115.

4 Edelman RR. Clinical magnetic resonance imaging: Chicago Metropolitan Area: Saunders Elsevier; 2006.

5 Fornasa F, Nesoti MV, Bovo C, Bonavina MG. Diffusion-weighted magnetic resonance imaging in the characterization of axillary lymph nodes in patients with breast cancer. J Magn Reson Imaging 2012; 36:858–864.

6 Kamitani T, Hatakenaka M, Yabuuchi H, Matsuo Y, Fujita N, Jinnouchi M, *et al.* Detection of axillary node metastasis using diffusion-weighted MRI in breast cancer. Clin Imaging 2013; 37:56–61.

7 Mohsen O, Fereshteh N. An extended VIKOR method based on entropy measure for the failure modes risk assessment–a case study of the geothermal power plant (GPP). Safety Sci 2017; 92:160–172.

8 Razek AAKA, Lattif MA, Denewer A, Farouk O, Nada N. Assessment of axillary lymph nodes in patients with breast cancer with diffusion-weighted MR imaging in combination with routine and dynamic contrast MR imaging. Breast Cancer 2016; 23:525–532.

9 Chung J, Youk JH, Kim J-A, Gweon HM, Kim E-K, Ryu YH, *et al.* Role of diffusion-weighted. An extended VIKOR method based on entropy measure for the failure modes risk assessment–A case study of the geothermal power plant (GPP). Safety Sci 2017; 92:160–172.

10 Ismail AAA, Hasan DI, Abd-Alshakor H. Diagnostic accuracy of apparent diffusion coefficient value in differentiating metastatic form benign axillary lymph nodes in cancer breast. Egypt J Radiol Nucl Med 2014; 45:1011–1016.

11 Ganz PA, Yip CH, Gralow JR, Distelhorst SR, Albain KS, Andersen BL, *et al*. Supportive care after curative treatment for breast cancer (survivorship care): resource allocations in low-and middle-income countries. A Breast Health Global Initiative 2013 consensus statement. Breast 2013; 22:606–615.

12 Wang J, Liao Q, Zhang Y, Yu C, Bai R, Sun H. Differential diagnosis of axillary inflammatory and metastatic lymph nodes in rabbit models by using diffusion-weighted imaging: compared with conventional magnetic resonance imaging. Korean J Radiol 2012; 13:458–466.

13 Vandecaveye V, De Keyzer F, Vander Poorten V, Dirix P, Verbeken E, Nuyts S, *et al*. Head and neck squamous cell carcinoma: value of diffusion-weighted MR imaging for nodal staging. Radiology 2009; 251:134–146.

14 Koh D-M, Collins DJ. Diffusion-weighted MRI in the body: applications and challenges in oncology. Am J Roentgenol 2007; 188:1622–1635.

15 Yamaguchi K, Schacht D, Nakazono T, Irie H, Abe H. Diffusion weighted images of metastatic as compared with nonmetastatic axillary lymph nodes in patients with newly diagnosed breast cancer. J Magn Reson Imaging 2015; 42:771–778.

16 Zhang F, Zhu L, Huang X, Niu G, Chen X. Differentiation of reactive and tumor metastatic lymph nodes with diffusion-weighted and SPIO-enhanced MRI. Mol Imag Biol 2013; 15:40–47.